Overview of the US collaborative program in stellarator experiments*

D. A. Gates[1], C. Baylard[4], J. Baumgaertel[1], M. Bitter[1], A. Boozer[1], H.-S. Bosch[4], T. Bräuer[4], T. Brown[1], M. Cole[2], D. Darrow[1], T. Dodson[1], P. J. Fogarty[2], M. Goto[3], W. Guttenfelder[1], R. Haange[4], G. Hammett[1], J. H. Harris[2], P. Heitzenroeder[1], K. Hill[1], K. Ida[3], M. Isobe[3], T. Klinger[4], R. König[4], L.-P. Ku[1], S. Lazerson[1], D. R. Mikkelsen[1], S. Morita[3], H. Neilson[1], K. Ogawa[5], N. Pablant[1], N. Pomphrey[1], A. Reiman[1], S. Sakakibara[3], R. Sanchez[2], C. H. Skinner[1], B. Stratton[1], Y. Suzuki[3], K. Tanaka[3], L. Wegener[4], A. Werner[4], R. Wolf[4], P. Xanthopoulos[4], H. Yamada[3], M. Yosinuma[3], M. Zarnstorff[1]

[1] Princeton Plasma Physics Labortory, Princeton, NJ USA
[2] Oak Ridge National Laboratory, Oak Ridge, TN USA
[3] National Institute for Fusion Science,Toki, Japan
[4] Max-Planck Institute for Plasma Physics, Greifswald, Germany
[5] Graduate University for Advanced Study, Toki, Japan

E-mail contact of main author: dgates@pppl.gov

Abstract. The US collaborative program in stellarator experiments is summarized, including results from and contributions to both W7-X and LHD. Specific results from LHD include: equilibrium reconstruction, diagnostic development, fast particle physics, and high beta research. These research topics reflect areas of strength for the US program and also are areas of synergy with the priorities of the LHD research activity. Recent results from each of these areas will be presented including: lost fast-ion data during Alfvènic activity, analysis of beta limiting instabilities, and progress towards data based equilibrium reconstruction. Contributions to W7-X, which is still under construction, are dominated by fusion engineering activities. These activities include: design of and assembly plans for the installation of the high temperature superconducting leads for the modular coils on W7-X, and detailed collision analysis of installations of cooling lines within the W7-X cryo-stat. These activities, along with plans for the future, will be presented in the context of the goals of a reconfigured US experimental stellarator program.

1. Introduction

Recently, the US national experimental stellarator program has shifted from being a construction program largely focused on development of a Proof-of-Principle scale research facility, to one focused on collaborative efforts. This paper presents the status of this redirected program. The primary activities advance the stellarator concept through participation in the research programs of the Large Helical Device (LHD) at the National Institute for Fusion Science in Toki, Japan, and Wendelstein 7-X (W7-X) at the Max-Planck Institute for Plasma Physics in Greifswald, Germany.

2. Collaborations at the National Institute for Fusion Science (NIFS)

Collaborative activities at the Large Helical Device encompass a broad range of research activities including: high beta research, diagnostic development, fast particle physics, and equilibrium reconstruction without the assumption of nested flux surfaces. These research topics reflect areas of strength for the US program and also are areas of synergy with the priorities of the LHD research activity.

2.1 LHD High β-research

Given the recent success on LHD in achieving high β plasmas [1], it is natural to investigate what physics is determining the operational β-limit. To this end a series of experiments has been proposed that aims to investigate the parametric dependencies of the observed β-limit. One such experiment involved the application of varying amounts of neutral beam driven current to change the shear in the profile of the rotational transform and then applying

substantial heating power to probe the β-limit. The results of this scan are shown in Figure 1, which plots the maximum achieved plasma beta versus the plasma current in the co-direction. There is a clear nearly linear reduction in the value of β that is achieved.

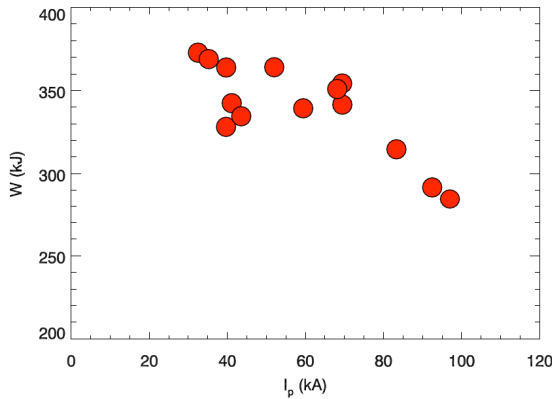The profiles of electron pressure from Thomson scattering [2], from a time just before the time of maximum β, are shown in Figure 2a for a subset of the data from Figure 1. The subset was selected in such a way so the electron density at the time of maximum β was comparable for each of the shots (total variation of the electron density was <10%) while maintaining near full range of variation in the plasma current and β.

The variation in the ι profile due to the increase of the neutral beam driven current is constrained by the Motional Stark Effect diagnostic [3], which provides a measure of the pitch local magnetic field at numerous locations within the LHD plasma. The MSE measurement constraint is applied through a procedure described in reference [4]. A comparison of the constrained profiles for the same series of
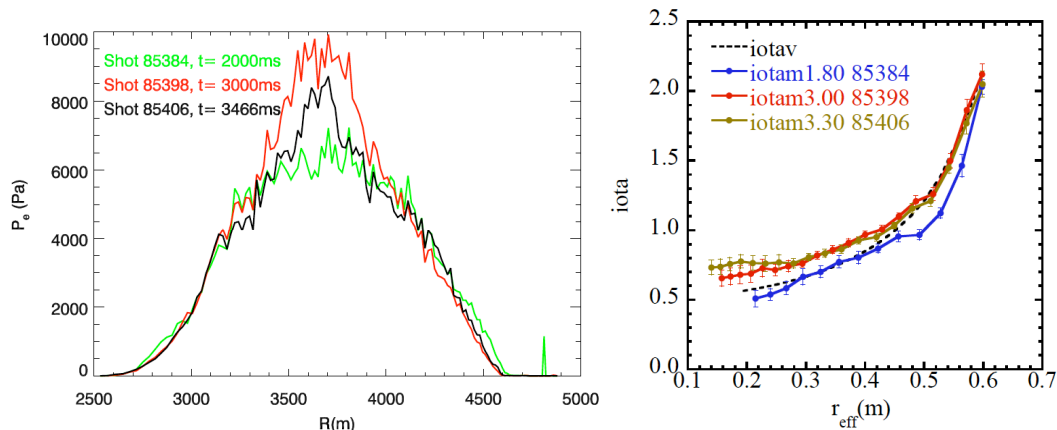
Figure 1: a) plot of the maximum stored energy vs. plasma current for the shots from an experiment designed to test the β-limit as a function of plasma current on LHD

Figure 2: a) Electron pressure profile for 3 shots at different currents just before the pressure collapse a) I_p = 40.0kA (85384) b) I_p = 69.5kA (85398) c) I_p = 92.5kA (85406) b) the ι profile, as constrained by MSE measurements. The dashed line is the vacuum ι. The times of the Thomson scattering measurements were chosen so that they were as close as possible to the time of maximum stored energy.

discharges is shown in Figure 2b. As can be seen from the figure, the effect of the increasing plasma current is to raise the central ι, as expected. It is also clear that, as the central ι increases, the core shear decreases, due to the strong peaking of the neutral beam driven current.

With the information from both the MSE constrained ι profiles and the shape of the pressure profiles, there are some interesting features that can be observed: 1) the even parity island which is apparent in the core of the highest current discharge, which has $\iota = 0.75$ within large low shear region in the core, visibly diminishes 2) The electron pressure and the pressure gradient in the neighborhood of the flat spot on small major radius side of the profile (which is consistent with the location of the 1/1 island) is the same for each discharge, even though the global parameters vary significantly. It is apparent that the overall shape of the pressure

profile at the β-limit is evolving strongly as a function of plasma current, but it is possible that the limit is determined by the pressure gradient across the 1/1 surface reaching a reproducible critical value.

Just prior to the time of maximum β, an MHD mode with frequency in the range 4-6kHz is observed in magnetic diagnostics. This mode grows on a several hundred-millisecond time scale, which is not consistent with ideal MHD mode growth. It could be a non-linearly saturated mode, or a resistive mode. Work is ongoing to identify this mode including but not limited to: identification of the radial eigenfunction, determination of the ideal stability for the observed profiles.

2.2 LHD Diagnostic development: Imaging X-ray crystal spectrometer

As part of the PPPL-NIFS collaboration program a new x-ray imaging crystal spectrometer will be installed on LHD to record spatially and time resolved x-ray line spectra of helium-like argon. The objectives of this collaboration project are twofold: (1) to provide a diagnostic for measurements of the ion-temperature and electron-temperature profiles which is independent of neutral beam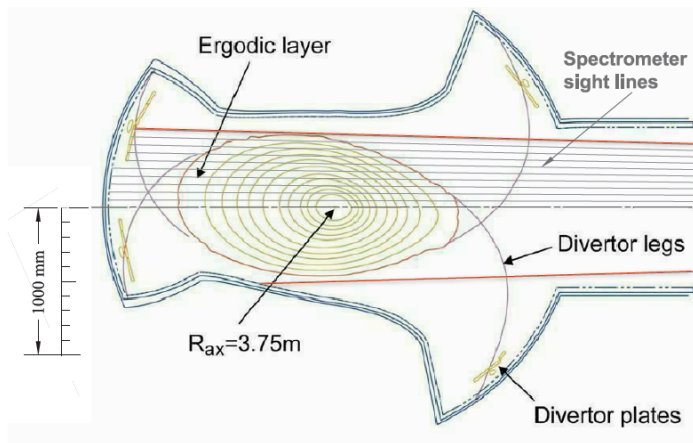 injection and which provides data for all experimental conditions, including long-pulse plasmas; and (2) to apply the stellarator equilibrium reconstruction codes, STELLOPT and PIES, which are being developed at PPPL, to the analysis of these spectral data and, in general, data from LHD diagnostics.

Figure 3: Plasma cross-section with contour plots of constant magnetic flux tubes and sightlines of the x-ray imaging crystal spectrometer being built for LHD. Lower half sightlines are not shown for clarity.

The spectrometer [5] will consist of a spherically bent 110-quartz crystal, with a radius of curvature of 5.890 m and an area of 100 mm (height) x 40 mm (width), and a spatially resolving, two-dimensional, Pilatus detector. The crystal will have an unimpeded view of the entire plasma, whose cross-section at the assigned equatorial access port is elliptical, with a vertical minor radius of 1 m perpendicular to the toroidal field. The center of the plasma will be at a distance of 18.733 m from the crystal, and the length of the crystal-detector arm will be 4.735 m, so that it will be possible to image a 1m high plasma onto the detector - a PILATUS 300K-W detector with total sensitive area of 254 x 35 mm^2 - with a demagnification of 0.253. Figure 3 shows the cross-section of the plasma with contours of constant flux surfaces and an arbitrary number of spectrometer sightlines (which are 5 cm apart at the plasma center) in the upper half of the plasma. Sightlines through the lower half of the plasma are not shown only to assure visibility of the constant flux contours. The two red lines represent the outermost sightlines of the spectrometer. The spatial resolution at the center of the plasma, given by the width and height of the crystal and the Bragg angle of 53.5°, is less than 2 cm vertically and less than 12 cm horizontally. Note that the spatial resolution can be improved by covering parts of the crystal area with an appropriate mask.

2.3 Fast particle loss measurements

Another area of historical concern for stellarators in general is fast ion confinement. Numerical design tools and operational experience were contributed to the design and implementation of a scintillator based fast-ion loss probe on LHD, similar in design to a detector first used on TFTR [6] (see Figure 4b). The detector is capable of determining the fast ion distribution function at the entry slit, resolving both pitch angle and energy.
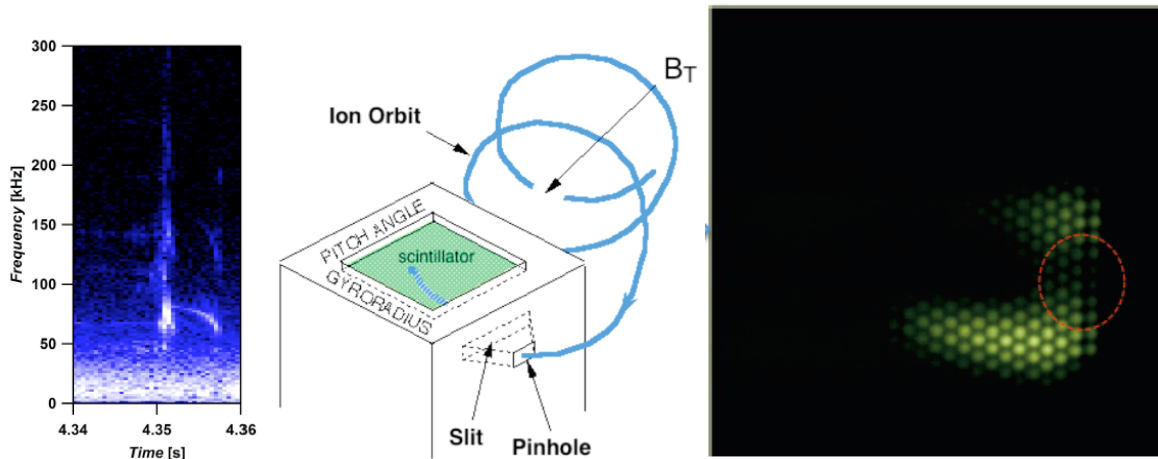

Figure 4: a) Spectrogram of a Mirnov coil showing the chirping mode, b) Schematic representation of the fast-ion loss probe, and c) results showing particles from transition orbits observed during the mode (region indicated by the red circle). The axes of the image are nearly linear with pitch angle (vertical) and energy (horizontal), as described in reference [6], with light intensity proportional to particle flux.

Measurements of fast ion losses from LHD plasmas during bursts of Alfvénic activity have been made with this scintillator type detector located on the large major radius side of the plasma. Several 180 kV H neutral beams are injecting into the discharges. Evident are repeated short bursts of activity in the 50-200 kHz frequency range, which is consistent with the frequencies for Alfvén eigenmodes. Figure 4a shows one of these bursts on an expanded time scale, showing a short broadband burst followed by a mode that sweeps down in frequency.

The image recorded by the fast ion loss probe's camera during a quiescent period between bursts shows fast ion loss at two different pitch angles, with both spots having gyroradii consistent with 180 kV H at the probe's position. The observed pitch angles, 43° and 59°, correspond to those of passing and trapped orbits, respectively. These appear to be prompt losses due to the magnetic structure of the discharge and the beam deposition profile. Interestingly, during the chirping mode, loss is seen in the range of pitch angles intermediate between the passing and trapped particle losses. This is depicted in Fig. 4c. These pitch angles correspond to transition orbits [7], which have large radial orbit deviations and thus can be easily lost from the discharge.

The mechanism which populates these orbits has not been investigated in any detail. The simplest process would be for a population of passing particles to lose energy through interactions with the chirping mode, causing them to convert to transition orbits. However, the image sequence from the camera suggests that the pitch angle range of trapped particle loss may progressively extend toward the passing particle pitch angle during the chirping mode. This would indicate the mode is adding parallel energy to these lost ions or extracting perpendicular energy.

2.4 Equilibrium reconstruction

An effort is underway to develop generalized equilibrium reconstructions which do not rely on the assumption of nested flux surface for the Large Helical Device. The project is progressing through the implementation of diagnostic data in various codes developed for investigation of magnetic equilibrium in toroidal devices. A detailed description of the magnetic coils for the device along with the locations of diagnostic measurements has been incorporated, as shown in Figure 5a. This allows for implementation of synthetic diagnostics in the various equilibrium codes (VMEC, PIES, HINT2). Recently the DIAGNO routine [8] has been upgraded to provide synthetic diagnostics for the LHD device. This now allows full reconstruction of LHD fields under the assumption of good nested flux surfaces with VMEC [9]. Treatment of stochastic regions and magnetic islands requires the implementation of these diagnostic for the PIES [10] and HINT2 codes [11]. These codes are currently undergoing benchmarking.
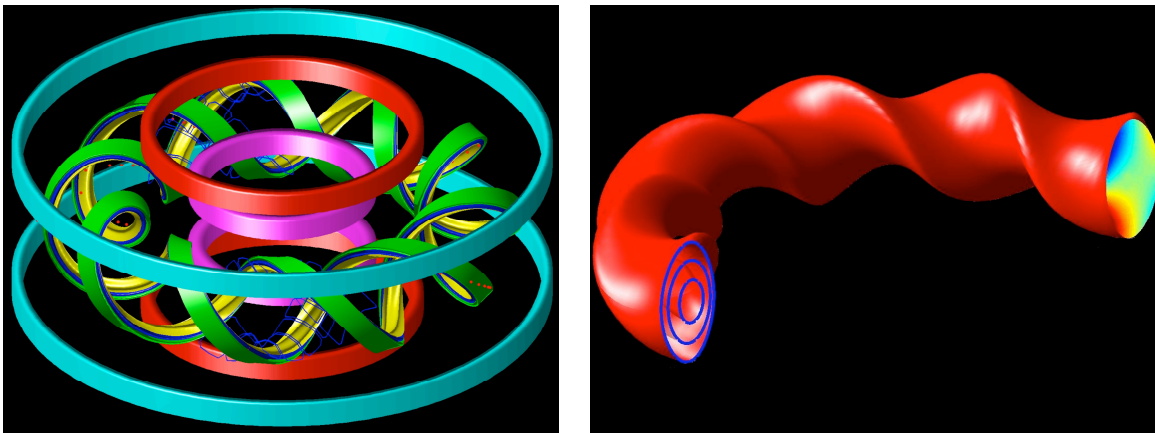

Figure 5: a) LHD Magnetic Coils and diagnostic probes configuration. The helical coil configuration (green, yellow and dark blue) the poloidal coils (red, purple, and light blue). The saddle loops are the dark blue lines draping across the helical coils. b) LHD VMEC vacuum equilibrium solution. The contour plot on the right indicates |B| while the outline of three flux surfaces are indicated on the left.

The LHD reconstruction effort is currently focused on validation of the synthetic magnetic diagnostics (DIAGNO) against actual measurements and benchmarking of stochastic behavior between PIES and HINT2. The VMEC code has found a vacuum equilibrium, shown in Figure 5b, which is used to calculate synthetic diagnostics for comparison to vacuum shot data from the LHD device. The benchmarking of the PIES code against the HINT2 code is currently examining the parallel current calculated in stochastic regions. This is being done to help elucidate differences between equilibria found for W7-X stellarator.

3. Collaborations with the IPP-Greifswald

In addition to activities on LHD, US stellarator researchers have also been collaborating with the W7-X team. Since W7-X is still under construction, the US efforts to date have included engineering and construction activities, which also have applications to ITER. Work has also proceeded with work aimed at advancing turbulence calculations in stellarator geometry, which is part of a broader international stellarator turbulence research activity.

3.1 Benchmarking of GS2 in stellarator geometry

As a first important step toward applying the GS2 gyrokinetic stability and turbulence simulation code to stellarator configurations, PPPL and IPP are benchmarking the GS2 and GENE codes. This activity actually began when GENE was developed, for a simplified

axisymmetric model configuration, and was renewed when GENE was extended to an arbitrary geometry [12]. Previous to this development, the stellarator geometry used by GS2 [13] was modeled very closely on Rewoldt's pioneering work [14]. Before tackling the stellarator benchmark, a realistic, shaped tokamak equilibrium was chosen as a case of intermediate complexity [15]. The IPP geometry interface code, GIST [16], which provides the required geometrical input for the gyrokinetic solver, is straightforward to operate, and together with the modular character of GS2 has enabled us to readily use GIST output as the geometrical foundation for GS2 calculations. After the benchmarks with the older GS2 geometrical codes are completed, we plan to use GIST exclusively with GS2 in the future.

Our first benchmark of a stellarator configuration is based on the S3 standard plasma of the NCSX design, and all the geometrical terms (see [14] for details) calculated for GS2 and for GENE agree to within ~1%. The algorithms used to determine the geometrical coefficients are independently coded and follow fundamentally different methods, but produce very consistent results. The mode frequencies and linear growth rates of Ion Temperature Gradient (ITG) modes (with adiabatic electrons) also compare well, see Figure 6. The
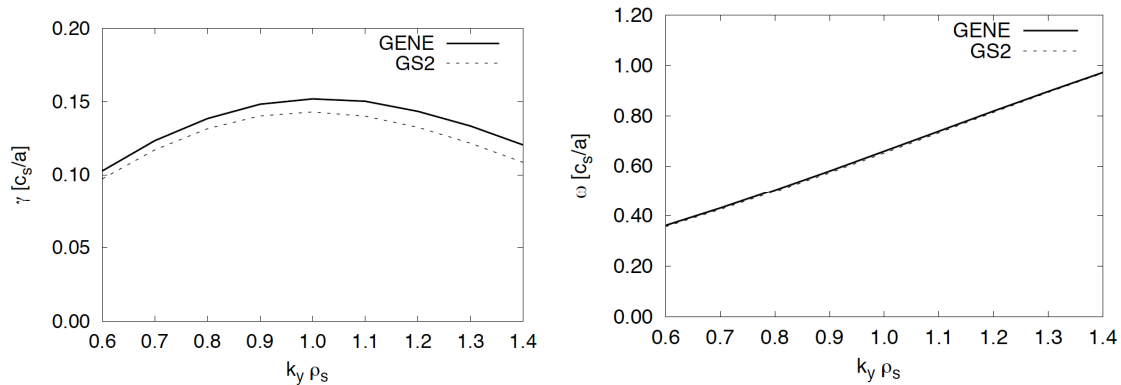

Figure 6: a) the growth rates (normalized with respect to c_s/a where c_s is the sound speed, a is minor radius) plotted vs. the $k_y\rho_s$ spectrum (here, $\rho_s = c_s/\Omega_i$, Ω_i is the ion Larmor frequency, and y is the binormal direction) and b) the real frequencies also vs. $k_y\rho_s$ spectrum.

agreement is excellent for small values of the binormal wavenumber $k_y\rho_s$, but grows moderately beyond the peak of the growth rate for smaller scales, and into the regime where Finite Larmor Radius (FLR) corrections become significant. This behavior is not peculiar to the stellarator stimulations, it is also typically seen in tokamak benchmarks and evidently reflects different methods of including FLR effects into the gyrokinetic codes.

This benchmark activity will eventually include W7-AS and W7-X configurations, and will touch upon linear stability for Trapped Electron Modes (TEM), combined ITG/TEM, finite collisionality, and electromagnetic effects. A similar benchmark activity will soon begin in collaboration with NIFS.

3.2 Engineering and configuration control

For the past year, a US team consisting of engineers from ORNL and PPPL has been working together with the W7X stellarator assembly team to design tooling and techniques for the precision assembly of the high current (17 kA) leads connecting the W7X stellarator coil set to the cables from the W7X power supply.

The task was to develop a scheme to lift and support the heavy (~500 kG) lead assemblies and align and hold them securely in position so the leads could be welded to the coil current feeds in five positions around the torus. The temporary supports must then be lowered and the loads shifted precisely to the permanent support structure without disturbing the joint itself. The working space in and near the lead fixing boxes is barely large enough for a technician's

arms, and the tolerances for placement of the leads are ~mm. The design work therefore has had to be carried out using 3D computer techniques supported by real world checks at ORNL and IPP using mockups of the relevant parts of the W7X device. The overall approach features a custom-built, movable lead installation cart with precision hydraulic positioners for the current feeds which can be used in a variety of configurations to translate, raise, position, support, and remove the lead assemblies as illustrated in Figure 7.

In addition to the lead assembly work, a full time engineer was assigned two major tasks in the important area of collision analysis. The first was to perform Module 5 cryogenic cooling pipe collision analysis using CATIA [17]. The second was a byproduct of the first and was to design a pilot project for a new software product called 3DCS [18].

A prior attempt was made for analyzing the cryo-pipes of Module 5, but proved to be too labor intensive. Thus, there was an agreement that the pipes would be installed with a minimum tolerance of 5mm. The Module 5 cryogenic cooling pipe check showed important deviations to the agreed tolerance chain. These findings were significant enough to warrant a detailed collision analysis of the cryogenic cooling pipes for the remaining four modules.

The 3DCS software was recommended as a possible replacement to the labor-intensive process that is currently in use at W7-X for collision analyses. In order to evaluate the usefulness and applicability of the software, a pilot project had to be designed for the software to attempt to mimic the current process and compare the results. The pilot project design was completed and the package has been delivered to the 3DCS consultant for testing.
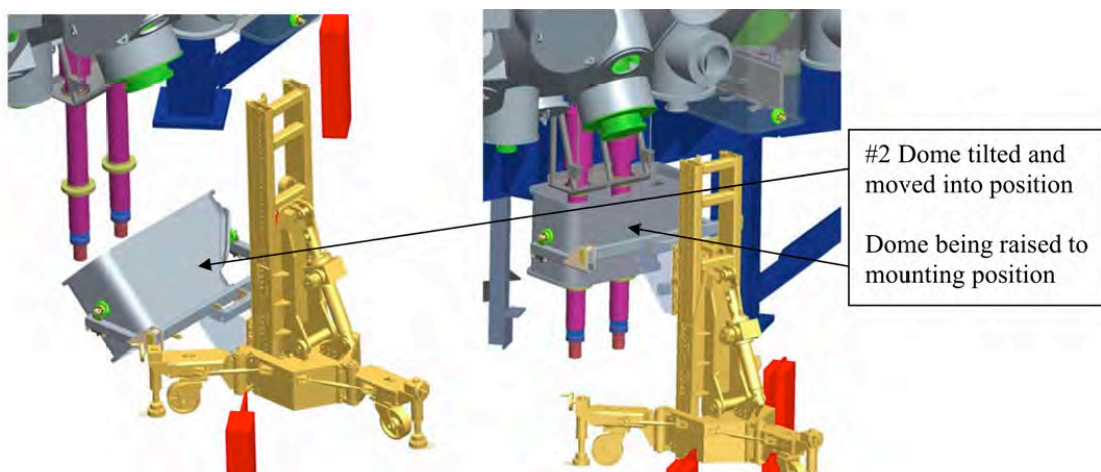

Figure 7: The US designed lead cart here being shown to position and install the dome which covers the high current superconducting leads underneath W7-X.

4. Future plans for collaboration

Future activities for collaborative activities with LHD include: full equilibrium reconstruction without the assumption of nested flux surfaces using the PIES and SIESTA equilibrium codes, further study of fast-ion confinement, real-time dust detection using dust detectors originally developed on NSTX, and confinement physics based on ion temperature profile measurements as provided by the x-ray crystal spectrometer currently under construction. In addition, there are opportunities for expended collaboration in the area of divertor physics. The W7-X collaboration is also envisioned to expand with major areas for potential future activities including the design of divertor trim coils, plasma control, and diagnostic development.

5. Summary and discussion

The US collaborative program in international stellarator experiments has made substantive contributions to numerous topical research areas that are of importance to stellarator physics. These areas include, lost fast-ion data during Alfvènic activity, analysis of beta limiting instabilities, diagnostic development aimed at determining confinement in regimes relevant to high β stellarators, and progress towards data based equilibrium reconstruction. Additionally, the US program has been successfully contributing its substantial engineering expertise, which was developed for the now cancelled NCSX program, towards solving the issues facing the W7-X device which is currently being constructed.

Fusion energy research is an increasingly international endeavor, with more and more research being performed within the context of multi-national teams. The US experimental stellarator program has recently shifted from a program focused on construction of a proof-of-principle scale experiment to one that focuses intensively on international collaboration. The US program is diverse with numerous areas of interest and expertise. This diversity will be maintained, but it is also necessary to develop initiatives that focus on solving explicit issues that are deemed high priority by the stellarator community. After substantial discussion within the US community - particularly within the context of the recent ReNeW activities - and also with our international partners, the US community has proposed to develop a research program to address 3D divertor science. It is hoped that with these refocused activities the US stellarator community can continue to be a vital component of international experimental stellarator research.

References

[1] S. Sakakibara, et al., Plasma Phys. Control. Fusion **50** (2008) 124014

[2] K. Narihara, K. Yamauchi, I. Yamada, T. Minami, K. Adachi, et al., Fusion Engineering and Design **34-35** (1997) 67

[3] K. Ida, M. Yoshinuma, K. Y. Watanabe, T. Kobuchi, and K. Nagaoka, Rev. Sci. Inst. **76**, (2005) 053505

[4]K. Ida, M. Yoshinuma, C. Suzuki, T. Kobuchi, K. Y. Watanabe, Fus. Sci. and Technology **58**, (2010) 383

[5] M. Bitter, K. Hill, D. Gates, D. Monticello, H. Neilson, Rev. Sci. Inst. **81**, (2010) 1

[6] S. Zweben, et al., Nucl. Fusion **30**, (1990) 1551

[7] Sanuki H., J. Todoroki, and T. Kamimura, Phys. Fluids B **2** (1990) 2155

[8] H. J. Gardner, Nucl. Fusion **30**, (1990) 1417

[9] S. P. Hirshman and J. C. Whitson, Phys. Fluids **26**, (1983) 3553

[10] A. H. Reiman and H. Greenside, Comput. Phys. Commun. **43**, (1986) 157

[11] Y. Suzuki, et al., Nucl. Fusion **46** (2006) L19

[12] P. Xanthopoulos and F. Jenko, Phys. Plasmas **13** (2006) 092301

[13] E. Belli, et al., "Gyrokinetic Microinstability Simulations in Stellarator Geometry", to be submitted to Physics of Plasmas

[14] G. Rewoldt, et al., Phys Plasmas **6** (1999) 4705

[15] P. Xanthopoulos, et al., Phys. Plasmas **15** (2008) 122108

[16] P. Xanthopoulos, et al., Phys. Plasmas **16** (2009) 082303

[17] For CATIA see: http://www.3ds.com/products/catia/portfolio/catia-v5/catia-v5r20/

[18] For information on 3DCS see: http://www.3dcs.com/pages/sw_ta_catia.php